J. Phys. Chem. A **1999,** *103,* 3923−3934

Ab Initio Quantum Chemical and Kinetic Modeling Study of the Pyrolysis Kinetics of Pyrrole

Muhamad Martoprawiro, George B. Bacskay,* and John C. Mackie*

School of Chemistry, University of Sydney, NSW 2006, Australia

Received: November 9, 1998; In Final Form: January 29, 1999

The kinetics of pyrolysis of pyrrole have been investigated theoretically by ab initio quantum chemical techniques and by detailed chemical kinetic modeling of previously reported experimental results. [Mackie, J. C.; Colket, M. B.; Nelson, P. F.; Esler, M. *Int. J. Chem. Kinet.* **1991**, *23*, 733.] The overall kinetics can be successfully modeled by a 117 step kinetic model that gives good agreement with temperature profiles of major products and also provides an acceptable fit for minor products. The thermochemistry and rate parameters of a number of key reactions have been obtained by ab initio calculations carried out at CASSCF, CASPT2, and G2(MP2) levels of theory. Several reaction pathways were investigated. The major product, HCN, arises principally from a hydrogen migration in pyrrole to form a cyclic carbene with the NH bond intact. Ring scission of this carbene leads to an allenic imine precursor of HCN and propyne. This is the decomposition pathway of lowest energy. Pyrolysis is preceded by the facile tautomerization of pyrrole to 2*H*-pyrrolenine. The latter can undergo CN fission to form an open chain biradical species, which is the precursor of the butenenitrile isomeric products, *cis*- and *trans*-crotononitrile and allyl cyanide. The biradical can also undergo facile H-fission to form cyanoallyl radical, which is an important precursor of acetylene, acetonitrile, and acrylonitrile. H_2 also arises principally from H-fission of the biradical.

Introduction

The five-membered heterocyclic pyrrole moiety is an important structure in coals and derived tars, and the thermal decomposition reactions of pyrrole are important for production of precursors of the oxides of nitrogen, NO_x, in the combustion of coals.

There have been four previous investigations of the kinetics of pyrolysis of pyrrole.[1−4] The last two of these are detailed kinetic studies using single pulse shock tube techniques to determine product distributions and rates of disappearance of reactant and of appearance of major products. In addition, the rate constant for disappearance of pyrrole has been measured behind reflected shocks by time-resolved absorption spectroscopy[4] as $k_{\mathrm{dis}} = 10^{14.1\pm0.6} \exp(-310 \pm 12\ \mathrm{kJ\ mol^{-1}}/RT)\ \mathrm{s^{-1}}$ over the temperature range of 1480−1680 K and at pressures between 7.5 and 13.5 atm. The foregoing Arrhenius parameters are not typical of those expected for direct ring opening of pyrrole to a biradical; hence Mackie et al.[4] postulated that pyrolysis was initiated by the reversible formation of pyrrolenine (2*H*-pyrrole) followed by ring scission to form a biradical intermediate (Py10) as follows:

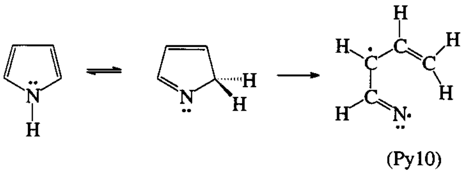

(1)

Mackie et al.[4] developed a detailed kinetic model based on this postulate to predict the major product profiles and reactant profiles. In that work, much of the thermochemistry was uncertain and estimates of thermochemical and kinetic parameters in the model were made by group additivity methods.[5] The basic premise of the model was that decomposition reactions of biradical Py10 led to the major isomeric products, *cis*- and *trans*-crotononitrile and allyl cyanide and also propyne and HCN. The origins of major products acetylene and acetonitrile were less obvious, and the importance (or otherwise) of pyrrolyl radicals which could arise from N−H fission of pyrrole could not be properly assessed.

To date, there has not been a rigorous theoretical test of the assumption that the initial tautomerization initiates pyrolysis, nor a detailed investigation of the reaction potential energy surface corresponding to the rearrangement and decomposition of the biradical Py10 that arises through C−N ring scission of the pyrrolenine tautomer. To remedy this situation we undertook a detailed ab initio quantum chemical study of the potential energy surfaces of a number of decomposition pathways, with a view to developing a more accurate and realistic kinetic model of the pyrolysis of pyrrole. As part of that work, we have carried out an ab initio study[6] of hydrogen fission from pyrrole and have computed the enthalpy of formation of the pyrrolyl radical. More recently, we characterized a low-energy decomposition pathway to propyne and HCN that proceeds via a cyclic carbene.[7] These studies, together with the present work, which includes further details of our ab initio quantum chemical study of the C_4H_5N reaction potential energy surface, has enabled the development of a realistic kinetic model that reproduces the experimental profiles[4] of the decomposition of pyrrole and of the formation of major products over the temperature range of 1300−1700 K and at pressures between 7.5 and 13.5 atm.

---

* Corresponding authors. E-mail for J.C.M.: j.mackie@chem.usyd.edu.au. E-mail for G.B.B.: bacskay@chem.usyd.edu.au.

10.1021/jp984358h CCC: $18.00

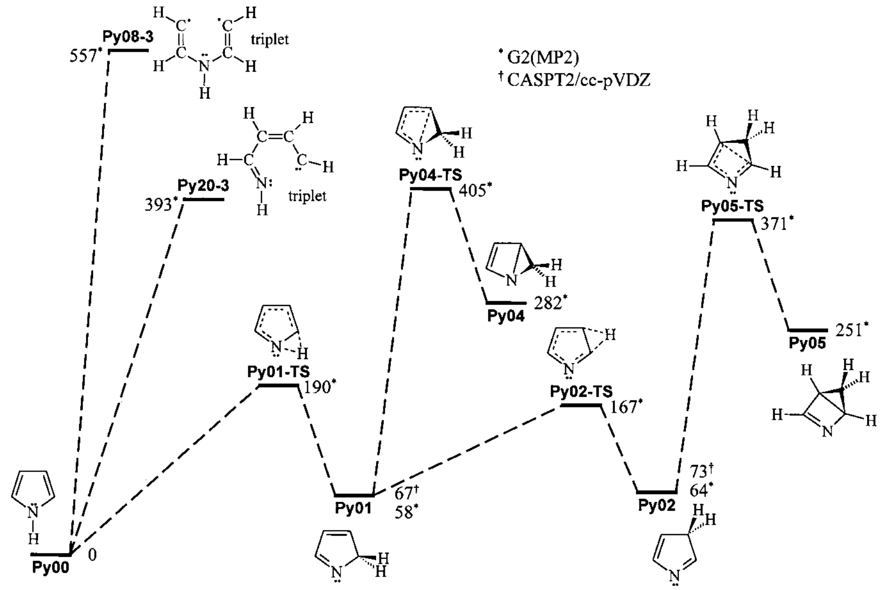

Figure 1. Potential energy surfaces for ring-opening reactions of pyrrole and its tautomerization to pyrrolenine and their subsequent bicyclization reactions at 0 K. (Energies in kJ mol^{-1} relative to pyrrole.)

Computational Methods

As in our previous work, the geometries and vibrational frequencies of the various species under study were computed using the Complete Active Space SCF (CASSCF) method,[8,9] in conjunction with the correlation consistent cc-pVDZ basis set.[10] Single point CASPT2 energy calculations,[11,12] with CASSCF wave functions as reference states, were then carried out at the equilibrium and transition state geometries, using the cc-pVDZ basis and, for selected systems, a valence triple-ζ basis with two sets of polarization functions (VTZ2P). The latter was derived from the cc-pVTZ basis, by removing the 4f and 3d polarization functions on the heavy atoms and hydrogens, respectively. The active orbital space in a given calculation was chosen to include all valence π molecular orbitals (MO) as well as a number of σ MO's that may be required to describe any bond breaking and making processes as well to accommodate nonbonding electrons. Thus, generally 8−12 active electrons were specified in active spaces of 7−11 orbitals.

The systems that could be adequately described by a single reference type wave function were also characterized at the G2(MP2) level of theory.[13] In some cases only the electronic energies were computed using G2(MP2), utilizing CASSCF/cc-pVDZ geometries and frequencies. The latter are scaled by a factor of 0.92 in the computation of zero-point energies and other thermodynamic quantities. In the current systems of interest such a choice of scale factor has been found to yield zero-point energies that are consistent with those based on SCF frequencies scaled by 0.893, as recommended in the original formulations of Gaussian-2 (G2)[13] as well as G2(MP2).

The calculation of thermal corrections to the molecular energies and hence enthalpies at specific temperatures was carried out using the standard formulas of statistical mechanics for quantum harmonic oscillators and classical rotors as well as classical translation.[14] Utilizing the computed barrier heights and molecular partition functions, the Arrhenius parameters of the reactions of interest were evaluated using Transition State Theory,[15] as described in our earlier paper.[6]

The quantum chemical calculations were performed using the DALTON,[16] MOLCAS2,[17] MOLCAS4,[18] GAUSSIAN94,[19] and GAUSSIAN98[20] programs on DEC alpha and IBM RS600/320 workstations.

Results and Discussion

General Considerations. An examination of the temperature profiles of major and minor products together with remaining pyrrole obtained in the earlier experimental study[4] shows that the butenenitrile isomers of pyrrole, viz., *cis*- and *trans*-crotononitrile and allyl cyanide as well as propyne and HCN all appear to be primary products and to be formed with approximately similar temperature dependences. Similar conclusions were also reached by Lifshitz et al.[3] who reported apparent activation energies of formation of these products to be around 305−350 kJ mol^{-1} and of values comparable with the activation energy for overall decomposition of pyrrole. Thus, in the ab initio calculations described below, we have searched for low activation energy pathways to these products.

Computational Results. The quantum chemical calculations on pyrrole and its isomers were undertaken with the aim of elucidating the mechanisms of decomposition. This implies a theoretical study of the pathways that were postulated by Mackie et al.[4] as well as exploring the feasibility of other reactions and pathways that had not been previously considered. In the course of this study the geometries, energies, and frequencies of over 100 distinct chemical species were computed using the ab initio techniques discussed in the previous section although only 64 of these contribute to the pathways discussed in this paper. The geometries and energies of these 64 species, as well as the rotational constants and vibrational frequencies of the molecules that comprise the important, viz., low-energy pathways, are summarized in Tables 1S−3S in the Supporting Information. In the main body of this paper the reaction energies and critical energies are given in the form of schematic molecular potential energy surfaces (PES) that also show, in a qualitative sense, the structures of the various molecular species and the codes assigned to them. All species are singlets, unless indicated otherwise.

Tautomerism of Pyrrole. The computed G2(MP2) energetics at 0 K of the tautomeric rearrangement between pyrrole and the pyrrolenines 2*H*- and 3*H*-pyrrole are shown in Figure 1. The barriers separating these tautomers are quite low, implying that at 1200 K and above, complete equilibration takes place. The thermal equilibrium among these species is, of course, an important part of the kinetic model.

There are other possible tautomers of pyrrole that result from the 1,2 migration of a hydrogen bonded to a carbon atom, either in pyrrole or in one of the pyrrolenines, yielding cyclic carbenes, some of which are shown below:

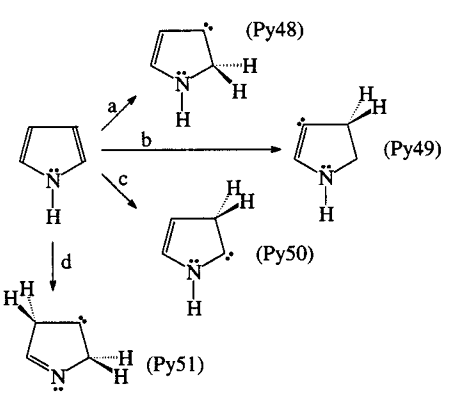

(2)

These carbenes are of course expected to be considerably less stable than the closed shell pyrrolenines. According to our G2(MP2) calculations, the heats of the above four reactions a, b, c, and d at 0 K are 265, 313, 203, and 349 kJ mol^{-1}, respectively, while the corresponding critical energies are 302, 327, 258, and 359 kJ mol^{-1}, indicating that the first three of these reactions could certainly occur at temperatures of 1300–1700 K. We will return to the discussion of these reactions when addressing ring-opening reactions as well as the overall decomposition reaction yielding HCN and propyne.

Ring Opening Reactions. Hypothetically, pyrrole could ring open by the fission of the NC or of a CC bond, resulting in NHCHCHCHCH, CHCHNHCHCH, or CHNHCHCHCH. An alternative, as proposed by Mackie et al.[4] on the basis of group additivity arguments, is the ring-opening reaction of pyrrolenine, yielding the $NCHCHCHCH_2$. Given the carbene or biradical nature of these open chain molecules, as well as those arising from other CC or CN bond fission reactions of both 2*H*- and 3*H*-pyrrole, it is expected that, for most of these, the ground electronic states would be triplets. Consequently, a quick estimate of the relative stabilities of these species can be carried out by single reference ab initio calculations, such as MP2 or MP4. These calculations and subsequent ones at the G2(MP2) level did in fact confirm that $NCHCHCHCH_2$ is the most stable isomer among the possible triplet biradicals by $\sim$90 kJ mol^{-1}. NHCHCHCHCH was found to be the second most stable triplet biradical. The energies of two triplet radicals that arise by the breaking of the CN or CC single bonds are also shown in Figure 1. Assuming that the corresponding singlet states would not be too dissimilar in energy, neither of these structures is expected to be of importance in the decomposition of pyrrole. The lowest energy products of ring-opening reactions of the two pyrrolenine tautomers are shown in Figures 2 and 3. Interestingly, the most stable molecule among these is singlet $CHNCHCHCH_2$ (Py31), which results from a CC bond fission of 2*H*-pyrrole. On the basis of G2(MP2) calculations the singlet ground state is 53 kJ mol^{-1} more stable than ${}^{3}A''$ $NCHCHCHCH_2$. Given the relatively high stability of Py31 and the low barrier to its formation, the subsequent rearrangement and decomposition of this species to HCN and propyne was also investigated, as indicated by the pathway in Figure 2. The feasibility of this route will be discussed in a later section of the paper.

The other important reaction on the singlet PES is the formation of the intermediate $NCHCHCHCH_2$ (Py10). The geometry of Py10 was computed to be planar and the bond lengths are consistent with the Lewis structure shown in Figure 2 and eq 1. Its spectroscopic state is ${}^{1}A''$; i.e., one of the open shell electrons occupies a π-type molecular orbital. The barrier to its formation is only $\sim$6 kJ mol^{-1} higher than the exothermicity of the reaction and therefore comparable with the barrier that leads to Py31, but substantially lower than the expected barriers associated with the formation of other open chain isomers of pyrrole.

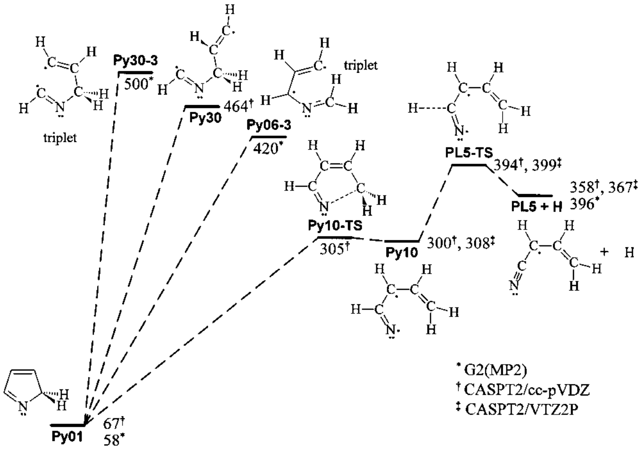

Figure 2. Potential energy surfaces for the ring-opening reactions of pyrrolenine and the formation of cyanoallyl at 0 K. (Energies in kJ mol^{-1} relative to pyrrole.)

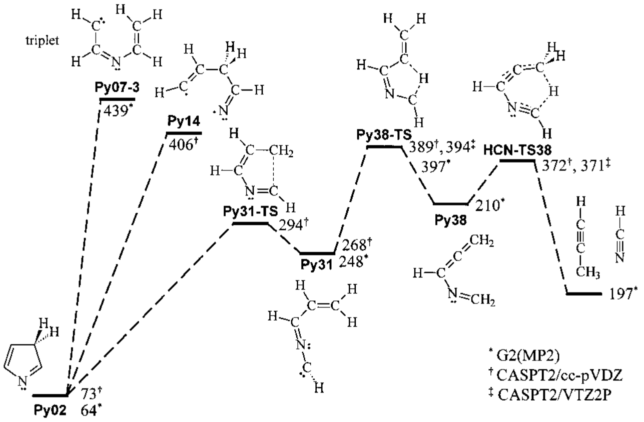

Figure 3. Potential energy surfaces for the ring-opening reactions of 3*H*-pyrrole (Py02) and the decomposition to HCN and propyne at 0 K. (Energies in kJ mol^{-1} relative to pyrrole.)

Formation of Cyanoallyl Radical. On the basis of previous studies[21] of reactions between acetonitrile and atomic hydrogen, as well as between HCN and a methyl radical, it is expected that the hydrogen attached to the cyano carbon in the open chain biradical Py10 would be only weakly bound. Consequently, the hydrogen loss reaction by Py10 to yield cyanoallyl (PL5) is of potential importance in the kinetic model. According to the CASPT2/VTZ2P energy calculations, the reaction is 65 kJ mol^{-1} endothermic while the barrier height (relative to Py10) is $\sim$92 kJ mol^{-1}, as shown also in Figure 2. These values are comparable to the corresponding energies of 85 and 118 kJ mol^{-1} associated with the reaction $CH_3HCN \rightarrow CH_2HCN + H$.[21] However, the G2(MP2) energy of the cyanoallyl + hydrogen system (relative to pyrrole) appears to be 29 kJ mol^{-1} higher than predicted at the CASPT2/VTZ2P level. Nearly half of this discrepancy (12 kJ mol^{-1}) can be traced to the contribution of the empirical "higher level correction" in the G2(MP2) energies, the rest (17 kJ mol^{-1}) being due to the basis set correction term of G2(MP2) as well as its more exhaustive treatment of electron correlation by the QCISD(T) method. In light of the above discrepancy, one may reasonably expect that

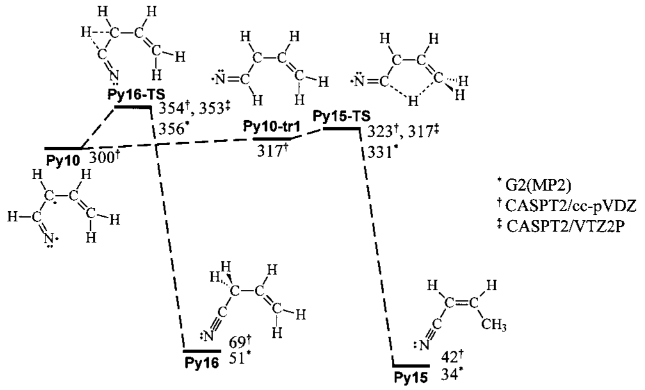

Figure 4. Potential energy surfaces for the formation of *cis*-crotononitrile and allyl cyanide at 0 K. (Energies in kJ mol^{-1} relative to pyrrole.)

the energy of the transition state PL5-TS could also have been underestimated by the CASPT2 calculations by ~15 kJ mol^{-1}. Given that PL5-TS, like Py10, is a singlet biradical, its energy cannot be computed by a single-reference technique such as quadratic CI. In the absence of a more reliable value, in the kinetic model the CASPT2 value for the barrier height is used with the proviso that a higher value may be justified if a better fit is sought.

The heat of formation of cyanoallyl, which is an important aspect of the kinetic model, was obtained from the computed [G2(MP2)] heats ($\Delta_r H^\circ_{298}$) of the isodesmic reactions

$$CH_2CHCHCN + CH_4 \rightarrow CH_2CHCH_2CN + CH_3 \quad (3)$$

$$CH_2CHCHCN + CH_2CHCH_3 \rightarrow CH_2CHCH_2CN + CH_2CHCH_2 \quad (4)$$

and experimental heats of formation ($\Delta_f H^\circ_{298}$) of the other species in the reactions. (For CH_4, CH_3, CH_2CHCH_2CN, CH_2CHCH_3, and CH_2CHCH_2, the measured heats of formation are -74.9,[22] 146.9 ± 0.8,[23] 157.7,[24] 20.4,[25] and 171.1 ± 2.9 [22] kJ mol^{-1}, respectively.) The resulting heats of formation of cyanoallyl are then computed to be 285.9 and 285.1 kJ mol^{-1}. If the CH bond breaking reaction of allyl cyanide, viz.

$$CH_2CHCH_2CN \rightarrow CH_2CHCHCN + H \quad (5)$$

is used, the resulting G2(MP2) heat of formation of cyanoallyl is 288.8 kJ mol^{-1}. This is consistent with the values obtained above and implies that the heat of the above bond breaking reaction is quite reliably estimated by G2(MP2).

Formation of cis-Crotononitrile and Allyl Cyanide. The open chain biradical Py10 will readily undergo hydrogen transfer reactions that result in the formation of two highly stable butenenitrile isomers of pyrrole, *cis*-crotononitrile, and allyl cyanide, as shown in Figure 4. *cis*-Crotononitrile is formed by a 1,4 H-transfer, after a low-energy conformational change in Py10, while allyl cyanide arises as a result of a simple 1,2 H-transfer in Py10. The critical energies of these reactions relative to Py10 at 0 K are very low: 23 and 53 kJ mol^{-1}, respectively, when computed at the CASPT2/cc-pVDZ level. As will be discussed later, however, the formation of these two products should be considered relative to pyrrolenine as reactant, since Py10 is not expected to equilibrate to any significant degree in the course of the reaction. While all three calculations, viz. CASPT2/cc-pVDZ, CASPT2/VTZ2P, and G2(MP2), are consistent with respect to the height of the barrier to the formation of allyl cyanide, the same appears not to hold in the case of the barrier height associated with the formation of *cis*-crotononitrile, varying from 317 kJ mol^{-1} (CASPT2/VTZ2P) to 331 kJ mol^{-1} (G2(MP2)), relative to pyrrole. This discrepancy is almost entirely due to the effect of the correction term in the G2(MP2) procedure for basis set incompleteness, estimated by the difference in MP2/6-311+G(3df,2p) and MP2/6-311G(d,p) energies. Assuming that this can be adequately done at the MP2 level, we conclude that the G2(MP2) estimate of the barrier height is likely to be more reliable than what had been obtained by the smaller basis CASPT2 calculations.

From the G2(MP2) data the following heats of reactions were calculated:

$$\text{pyrrole} \rightarrow \text{allyl cyanide } \Delta_r H^\circ_0 = 50.9 \text{ kJ mol}^{-1}, \quad \Delta_r H^\circ_{298} = 54.6 \text{ kJ mol}^{-1} \quad (6)$$

$$\text{pyrrole} \rightarrow cis\text{-crotononitrile } \Delta_r H^\circ_0 = 34.2 \text{ kJ mol}^{-1}, \quad \Delta_r H^\circ_{298} = 38.2 \text{ kJ mol}^{-1} \quad (7)$$

The heats of these reactions at 298 K, as computed from the experimental heats of formation,[24,26] are 49.4 and 25.7 kJ mol^{-1}, respectively. Thus, the agreement between the ab initio and experimental data is reasonable, although the significantly larger discrepancy (12.5 kJ mol^{-1}) in the case of the pyrrole → *cis*-crotononitrile reaction seems somewhat surprising, especially in light of the good agreement between theory (39.4 kJ mol^{-1}) and experiment (41.5 kJ mol^{-1}) for $\Delta_r H^\circ_{298}$ of the pyrrole → *trans*-crotononitrile reaction (using the experimental value[27] of 149.8 kJ mol^{-1} for the heat of formation of *trans*-crotononitrile). Since ab initio methods are generally very reliable in resolving the relative energies of conformers and geometric isomers, the above discrepancy in the case of *cis*-crotononitrile suggests that the accepted experimental value[24] of 134 kJ mol^{-1} for its heat of formation may well be too low by ~ 10−15 kJ mol^{-1}.

After the initial submission of this manuscript, a paper appeared by Dubnikova and Lifshitz[28] that includes a theoretical study of this pathway using density functional, CASSCF, and QCISD(T) methods. Overall, their results are in reasonable agreement with ours, although their computed barriers, as well as the energies of the intermediates and products, relative to pyrrole are lower by ~10−20 kJ mol^{-1} than those obtained in this work. In most cases this can be traced to the use of a smaller basis set by Dubnikova and Lifshitz in the computation of energies at stationary points on the PES.

Formation of Hydrogen Cyanide and Propyne. A number of different pathways were explored in an attempt to find the one that would be consistent with the experimental findings that the decomposition products HCN and propyne are primary products, along with the butenenitriles, and that the activation energy of the overall disappearance of pyrrole is 310 ± 12 kJ mol^{-1}, as measured between 1300 and 1500 K at 12 atm pressure. The reaction pathway that appears to satisfy these requirement is one that starts with a cyclic carbene tautomer of pyrrole, followed by ring opening that results in a closed shell allenic imine intermediate. The latter readily undergoes a 1,5 sigmatropic hydrogen shift, generating HCN and propyne as products. Full details of this mechanism are being published separately.[7] For completeness, however, the PES of this pathway is given in Figure 5. From the barrier heights and the computed partition functions the rate-determining step was found to be the hydrogen migration that yields the cyclic carbene. The corresponding computed Arrhenius *A*-factor and activation energy at 1200 K are $10^{13.74}$ s^{-1} and 322 kJ mol^{-1}, respectively. A slightly different pathway that yields allene and HCN as

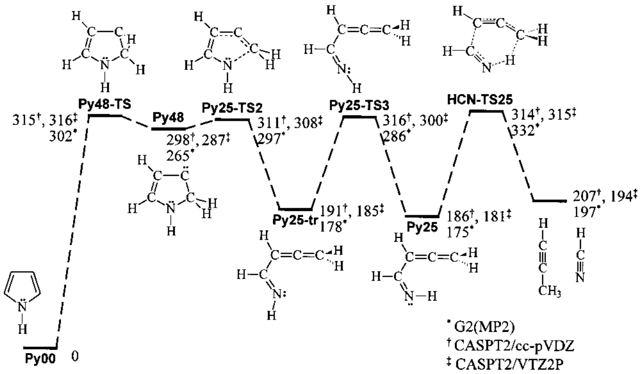

Figure 5. Potential energy surface for the formation of HCN and propyne via the cyclic carbene Py48 at 0 K. (Energies in kJ mol^{-1} relative to pyrrole.)

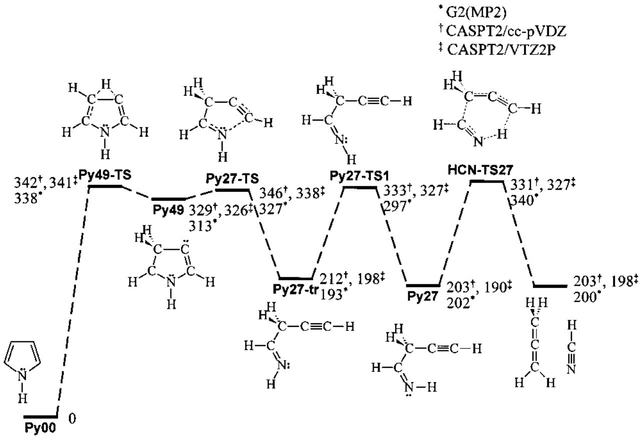

Figure 6. Potential energy surface for the formation of HCN and propyne via the cyclic carbene Py49 at 0 K. (Energies in kJ mol^{-1} relative to pyrrole.)

products are summarized in the PES in Figure 6. The small, yet significant, difference in barrier heights means that this second pathway is unlikely to compete with the previous one. Similar conclusions were reached concerning Py51 (see eq 2) as a possible intermediate.

The original proposal of Mackie et al.[4] was that the biradical Py10 would undergo a CC bond fission yielding HCN and the $CHCHCH_2$ carbene. Subsequent rearrangement of the latter would then yield allene or propyne. These two molecules are known to interconvert readily by a 1,3 H-transfer. The barrier to CC bond fission, computed at the CASPT2/cc-pVDZ level, is, however, much too high at 597 kJ mol^{-1} (relative to pyrrole) to allow this reaction to be considered as realistic. A large component of this barrier is the high endothermicity of the reaction yielding singlet $CHCHCH_2$, since relative to pyrrole the products are 458 kJ mol^{-1} higher in energy (at the G2(MP2) level). Even if intersystem crossing occurred, producing the above carbene in its triplet ground state, the reduction in the endothermicity of the reaction would be only ~28 kJ mol^{-1}, having calculated the singlet–triplet splitting in $CHCHCH_2$ by G2(MP2). In fact, with regard to the decomposition reaction

$$\text{pyrrole} \rightarrow \text{HCN} + C_3H_4 \qquad (8)$$

according to our G2(MP2) studies, there are only three possible isomers of C_3H_4 that could be considered as acceptable candidates on energetic grounds: propyne, allene, and cyclopropene. The corresponding G2(MP2) reaction energies at 0 K are 197, 200, and 296 kJ mol^{-1}. Therefore, when considering alternative pathways, in addition to the one discussed above,

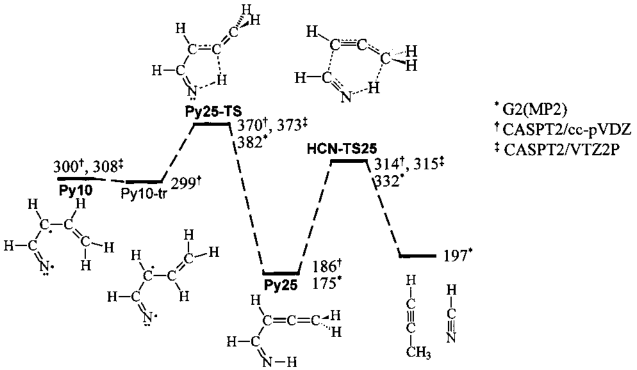

Figure 7. Potential energy surface for the formation of HCN and propyne from the open chain biradical Py10 at 0 K. (Energies in kJ mol^{-1} relative to pyrrole.)

Py10 or Py31 could be acceptable intermediates, provided both species undergo H-migration reactions such that the products of the subsequent decomposition reactions are HCN plus propyne, allene, or cyclopropene.

In the case of Py10 the above objective can be achieved, as shown in Figure 7, by forming Py10-tr, viz. a rotamer of Py10, followed by a 1,4-H migration that yields the imine Py25, which, as shown already, decomposes to HCN and propyne in a concerted reaction. While the critical energy of the H migration step is ~30–40 kJ mol^{-1} higher in an absolute sense than the one associated with the formation of the cyclic carbene, the large partition function of the transition state Py25-TS compared with that of pyrrolenine, makes the *A*-factor for this reaction approximately 1 order of magnitude larger than that for the reaction of pyrrole to HCN via the cyclic carbene. Consequently, the formation of HCN via Py25-TS is a reasonably important reaction in the kinetic model, at least at higher temperatures.

The alternative 1,2 H-transfers in Py10 producing $N{=}CH{-}CH_2{-}C{=}CH_2$ or $N{=}CH{-}CH{=}C{-}CH_3$, which may be considered reasonable precursors to the production of HCN plus allene or propyne on CC bond fission, were ruled out on energetic grounds. The energies of these two biradicals in their singlet states at 0 K, relative to pyrrole, were computed at the CASPT2/cc-pVDZ level to be 429 and 363 kJ mol^{-1}, respectively. For the latter system the transition state associated with the 1,2 H-transfer was located. Not unexpectedly, the reverse barrier height for the reaction was found to be very high: 175 kJ mol^{-1} at the CASPT2/cc-pVDZ level. Consequently, both of these mechanisms could be ruled out.

In the case of Py31 a 1,4 H-migration results in a stable closed shell intermediate, as shown in Figure 3, which then undergoes a 1,5 sigmatropic shift and decomposition. However, the critical energy of the first step is too high for this reaction to be of importance.

Cis–Trans Isomerization of Crotononitrile and Interconversion with Allyl Cyanide. According to the mechanism discussed thus far, pyrrole isomerizes to *cis*-crotononitrile. The trans isomer arises by a simple rearrangement reaction of the cis form, as elucidated experimentally by Doughty and Mackie.[29] This is believed to occur by internal rotation around the CC double bond that implies the breaking of the π bond and thus the formation of a biradical transition state. The CASPT2/cc-pVDZ calculations predict such a process to have a critical energy of 229 kJ mol^{-1} at 0 K on the singlet surface. The corresponding *A*-factor and activation energy at 1500 K were computed to be $10^{14.1}$ s^{-1} and 241 kJ mol^{-1}, respectively.

The mechanism for the isomerization of *cis*- and *trans*-crotononitrile to allyl cyanide and vice versa, as originally

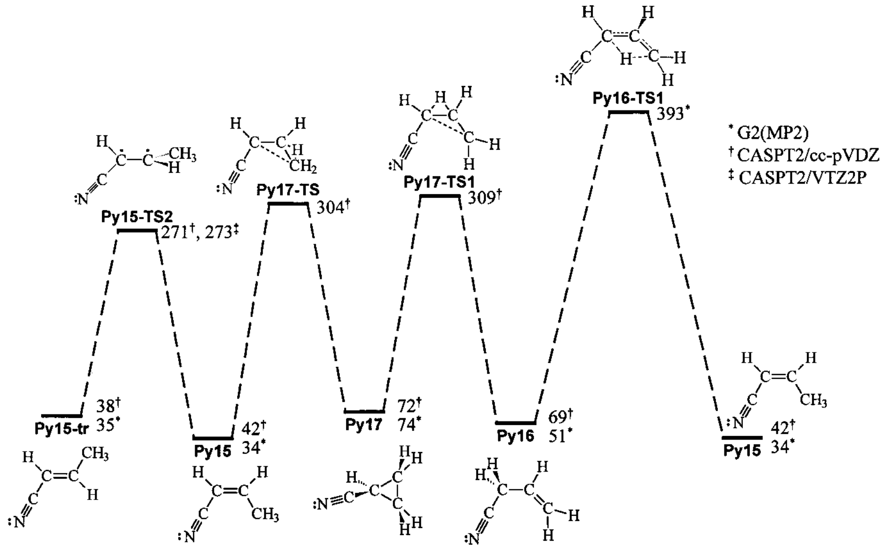

Figure 8. Potential energy surface for the interconversion between *trans-* and *cis*-crotononitrile and allyl cyanide at 0 K. (Energies in kJ mol^{-1} relative to pyrrole.)

established by Luckraft and Robinson,[30] is via cyclopropyl cyanide as the intermediate. Our calculated PES for the reaction involving *cis*-crotononitrile is shown in Figure 8, along with the single step *cis*−*trans* isomerization discussed above. Contrary to the suggestion of Luckraft and Robinson, no stable CH_2-CH_2CHCN biradical intermediate could be located between crotononitrile (Py15) and cyclopropyl cyanide (Py17) or between cyclopropyl cyanide and allyl cyanide (Py16). On the basis of their geometries, the two transition states Py17-TS and Py17-TS1 have every appearance of leading to the above biradical, but at the CASSCF level, at least, the geometries consistently collapsed to that of cyclopropyl cyanide. The computed Arrhenius *A*-factors and activation energies at 700 K (from the CASSCF/cc-pVDZ and CASPT2 data) for the isomerization of cyclopropyl cyanide to *cis-* and *trans*-crotononitrile and to allyl cyanide are $10^{14.62}$, $10^{14.84}$, and $10^{14.64}$ s^{-1} and 242, 247, and 246 kJ mol^{-1}, respectively, which compare reasonably well with the experimentally derived values of Luckraft and Robinson, viz. $10^{14.01}$, $10^{14.09}$, and $10^{14.59}$ s^{-1} and 237.6, 243.7, and 252.5 kJ mol^{-1}.

As our paper was being prepared for publication, a quantum chemical study of these reactions was published by Dubnikova and Lifshitz.[31] While their results are in qualitative agreement with ours, there are some notable differences between the two studies. The use of spin-unrestricted density functional and QCI methods by Dubnikova and Lifshitz for transition states and intermediates that are open shell singlet states results in a large degree of spin contamination and energies that are some average of singlet and triplet state energies. The presence of the triplet contamination would also confer a degree of stability on the CH_2CH_2CHCN biradical. According to our studies, using (spin-restricted) CASSCF, this biradical is predicted to be stable in its triplet state, but not as a singlet, as it collapses to cyclopropyl cyanide. We note, however, that the existence of such a *stable* biradical has no bearing on the computation of Arrhenius rate parameters.

An alternative mechanism, via a 1,3 H-transfer, has been studied, but the very high critical energy that has been computed for this reaction via the transition state Py16-TS1 (see Figure 8) effectively rules this channel out.

Formation of Hydrogen Cyanide and Allene from Cyclopropyl Cyanide. Given the high stability of cyclopropyl cyanide and its propensity for ring-opening reactions, as discussed above, the possibility of HCN elimination from this isomer was also investigated. This pathway and the computed energies are summarized in Figure 9. The first step is a concerted 1,2 H-transfer and ring opening reaction that results in the formation of the highly stable $CH_2C(CN)CH_3$ molecule (Py34), which may be expected to readily isomerize to $CH_2C(HCN)CH_2$ (Py35) by a 1,3 H-transfer. Py35 is a fairly stable biradical, with a planar geometry and hence a $^1A''$ ground state, with a high degree of electron delocalization that is manifested in the near-equal methylene to carbon CC distances. However, contrary to expectations, the barrier associated with the transition state Py35-TS is too high for this pathway to be seriously considered as an alternative to the one discussed previously, via transition state Py25-TS. Moreover, because Py35-TS is a tight transition state, the associated *A*-factor is also fairly low: ~$10^{13.8}$ s^{-1}. Interestingly, once Py35 is formed, it will readily dissociate to HCN and allene. An alternative to the above pathway, where a methylenic hydrogen in Py34 migrates to the cyano carbon, yielding $CHC(HCN)CH_3$ (which could readily dissociate to HCN and propyne) has a significantly higher critical energy, the transition state lying 420 kJ mol^{-1} above pyrrole. An even higher barrier (576 kJ mol^{-1} above pyrrole) is associated with the 1,2 H-migration in cyclopropyl cyanide, which would directly yield Py35.

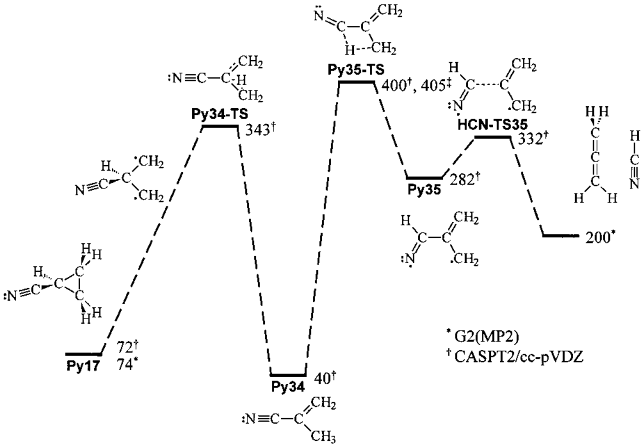

Figure 9. Potential energy surface for the formation of HCN and allene from cyanocyclopropene at 0 K. (Energies in kJ mol^{-1} relative to pyrrole.)

TABLE 1: Kinetic Model for Pyrrole Pyrolysis

	reaction[a]	A^b	n	$E_a{}^b$	ref
1	C_4H_5N+M ⇔ PYRLNE+M	1.2E+36	−5.5	239.5	PW/abin[c,d,e]
2	C_4H_5N ⇔ HNCPROP	1.1E+14	0	323.0	PW/abin
3	PYRLNE ⇔ ALLYLCN	3.5E+73	−16.5	478.6	PW/abin[d,e]
4	PYRLNE ⇔ *cis*-C_3H_5CN	1.4E+81	−18.8	474.5	PW/abin[d,e]
5	PYRLNE ⇔ HNCPROP	6.3E+61	−13.2	468.5	PW/abin[d,e]
6	PYRLNE ⇔ H+AC_3H_4CN	1.3E+79	−17.9	525.4	PW/abin[d,e]
7	HNCPROP ⇔ HCN+C_3H_4P	1.1E+13	0	151.7	PW/abin
8	*cis*-C_3H_5CN ⇔ *trans*-C_3H_5CN	1.4E+14	0	241.0	PW/abin
9	ALLYLCN ⇔ *cis*-C_3H_5CN	7.2E+14	0	246.4	PW/abin
10	ALLYLCN ⇔ *trans*-C_3H_5CN	7.0E+14	0	259.4	PW/abin
11	CH_3+HCCHCN ⇔ *trans*-C_3H_5CN	4.0E+13	0	0.0	29
12	CH_3+HCCHCN ⇔ *cis*-C_3H_5CN	4.0E+13	0	0.0	29
13	C_2H_3+CH_2CN ⇔ ALLYLCN	3.0E+13	0	0.0	29
14	*cis*-C_3H_5CN ⇔ HCN+C_3H_4P	2.6E+12	0.1	318.0	est
15	*trans*-C_3H_5CN ⇔ HCN+C_3H_4P	2.6E+12	0.1	318.0	est
16	H+ALLYLCN ⇔ C_2H_4+CH_2CN	5.0E+12	0	12.6	29
17	H+ALLYLCN ⇔ C_3H_5+HCN	3.5E+12	0	12.6	29
18	H+*trans*-C_3H_5CN ⇔ CH_3+H_2CCHCN	3.0E+12	0	25.1	29
19	H+*cis*-C_3H_5CN ⇔ CH_3+H_2CCHCN	3.0E+12	0	25.1	29
20	H+*trans*-C_3H_5CN ⇔ AC_3H_4CN+H_2	3.0E+13	0	20.9	PW
21	H+*cis*-C_3H_5CN ⇔ AC_3H_4CN+H_2	3.0E+13	0	20.9	PW
22	H+*trans*-C_3H_5CN ⇔ C_3H_4CN+H_2	3.0E+13	0	25.1	PW
23	H+*cis*-C_3H_5CN ⇔ C_3H_4CN+H_2	3.0E+13	0	25.1	PW
24	H+ALLYLCN ⇔ AC_3H_4CN+H_2	3.0E+13	0	20.9	PW
25	H+ALLYLCN ⇔ C−C_3H_4CN+H_2	3.0E+13	0	25.1	PW
26	AC_3H_4CN ⇔ C−C_3H_4CN	5.0E+13	0	217.6	29
27	C−C_3H_4CN ⇔ C_2H_2+CH_2CN	5.0E+13	0	117.2	PW
28	C_3H_5 ⇔ C_3H_4P+H	2.3E+13	0	251.9	29
29	C_3H_5+CN ⇔ ALLYLCN	3.0E+13	0	0.0	PW
30	CH_3+*trans*-C_3H_5CN ⇔ AC_3H_4CN+CH_4	1.5E+12	0	37.7	29
31	CH_3+*cis*-C_3H_5CN ⇔ AC_3H_4CN+CH_4	1.5E+12	0	37.7	29
32	CH_3+*trans*-C_3H_5CN ⇔ C_3H_4CN+CH_4	1.0E+12	0	46.0	29
33	CH_3+*cis*-C_3H_5CN ⇔ C_3H_4CN+CH_4	1.0E+12	0	46.0	29
34	CH_3+ALLYLCN ⇔ AC_3H_4CN+CH_4	1.5E+12	0	37.7	29
35	CH_3+ALLYLCN ⇔ C−C_3H_4CN+CH_4	1.5E+12	0	41.8	29
36	CH_2CN+ALLYLCN ⇔ AC_3H_4CN+CH_3CN	8.0E+11	0	37.7	29
37	CH_2CN+*trans*-C_3H_5CN ⇔ AC_3H_4CN+CH_3CN	1.0E+12	0	46.0	29
38	CH_2CN+*cis*-C_3H_5CN ⇔ AC_3H_4CN+CH_3CN	1.0E+12	0	50.2	29
39	HCCHCN+*trans*-C_3H_5CN ⇔ AC_3H_4CN+H_2CCHCN	1.0E+12	0	33.5	29
40	HCCHCN+*cis*-C_3H_5CN ⇔ AC_3H_4CN+H_2CCHCN	1.0E+12	0	33.5	29
41	HCCHCN+ALLYLCN ⇔ AC_3H_4CN+H_2CCHCN	7.0E+11	0	33.5	29
42	CH_3CN ⇔ CH_2CN+H	8.0E+14	0	397.1	21
43	CH_3CN ⇔ CH_3+CN	1.0E+15	0	489.5	21
44	H+CH_3CN ⇔ CH_3+HCN	1.0E+14	0	40.5	21
45	H+CH_3CN ⇔ CH_2CN+H_2	1.5E+13	0	41.8	21
46	2CH_2CN ⇔ SUCC	2.3E+13	0	0.0	21
47	H+AC_3H_4CN ⇔ ALLYLCN	5.0E+12	0	0.0	29
48	H+AC_3H_4CN ⇔ *cis*-C_3H_5CN	5.0E+12	0	0.0	29
49	H+AC_3H_4CN ⇔ *trans*-C_3H_5CN	5.0E+12	0	0.0	29
50	AC_3H_4CN ⇔ HCCCN+CH_3	1.0E+14	0	343.1	PW
51	C_3H_4CN ⇔ HCCCN+CH_3	6.0E+14	0	175.7	29
52	H+C_3H_4P ⇔ CH_3+C_2H_2	1.3E+05	2.5	4.2	38
53	CH_3+C_3H_4P ⇔ CH_4+C_3H_3	5.0E+11	0	36.8	39
54	CN+C_3H_4P ⇔ HCN+C_3H_3	1.0E+14	0	0.0	40
55	HCCHCN ⇔ HCCCN+H	1.0E+12	0	200.8	29
56	H+HCCHCN ⇔ H_2CCHCN	4.0E+13	0	0.0	29
57	H+H_2CCHCN ⇔ HCN+C_2H_3	5.0E+12	0	33.5	21
58	H+H_2CCHCN ⇔ HCCHCN+H_2	5.0E+13	0	33.5	29
59	H_2CCHCN ⇔ HCCCN+H_2	1.8E+12	0.2	318.0	21
60	H_2CCHCN ⇔ C_2H_2+HCN	2.6E+12	0.1	318.0	21
61	C_4H_4 ⇔ 2C_2H_2	1.5E+15	0	345.2	41
62	C_4H_4 ⇔ C_4H_2+H_2	2.0E+14	0	364.0	41
63	C_2H_5 (+M) ⇔ C_2H_4+H (+M)	2.0E+13	0	166.0	42
64	C_2H_4+M ⇔ C_2H_2+H_2+M	2.6E+17	0	331.8	42
65	C_2H_4+M ⇔ C_2H_3+H+M	2.6E+17	0	404.0	42
66	C_2H_4+H ⇔ C_2H_3+H_2	5.0E+13	0	33.5	43
67	H+C_2H_2 (+M) ⇔ C_2H_3 (+M)	1.0E+13	0	11.3	44, 21
68	2CH_3 (+M) ⇔ C_2H_6 (+M)	3.6E+13	0	0.0	41
69	C_2H_6+H ⇔ H_2+C_2H_5	5.4E+02	3.5	21.8	45
70	C_2H_6+CH_3 ⇔ CH_4+C_2H_5	5.5E−01	4	34.7	45
71	CH_3+H_2 ⇔ CH_4+H	6.5E+02	3	32.2	42
72	HCCHCN ⇔ C_2H_2+CN	5.0E+13	0	251.0	21
73	CN+H_2 ⇔ HCN+H	4.9E+05	2.4	8.9	45
74	C_2N_2+M ⇔ 2CN+M	1.4E+68	−13.2	715.9	40
75	H+C_2N_2 ⇔ HCN+CN	3.1E+14	0	32.9	21
76	CH_3+H (+M) ⇔ CH_4 (+M)	6.0E+16	−1	0.0	45
77	SUCC ⇔ $NCCHCH_2CN$+H	2.5E+15	0	400.4	21
78	$NCCHCH_2CN$ ⇔ H_2CCHCN+CN	2.2E+14	0	230.1	21
79	$NCCHCH_2CN$ ⇔ $C_4H_2N_2$+H	5.6E+13	0	198.7	21
80	$C_4H_2N_2$ ⇔ HCCCN+HCN	5.0E+13	0	309.6	21
81	CH_2CN+SUCC ⇔ CH_3CN+$NCCHCH_2CN$	3.5E+12	0	20.9	21
82	CH_3+SUCC ⇔ CH_4+$NCCHCH_2CN$	2.0E+12	0	20.9	21
83	H+SUCC ⇔ H_2+$NCCHCH_2CN$	3.0E+13	0	20.9	21
84	CN+SUCC ⇔ HCN+$NCCHCH_2CN$	5.0E+13	0	8.4	21
85	C_2H_5+H ⇔ CH_3+CH_3	1.0E+14	0	0.0	45
86	H_2+C_2H ⇔ C_2H_2+H	4.1E+05	2.4	3.6	46
87	C_2H_3+H ⇔ C_2H_2+H_2	4.0E+13	0	0.0	45
88	C_2H+C_2H_2 ⇔ C_4H_2+H	3.0E+13	0	0.0	46
89	C_2H_2+C_2H_2 ⇔ C_4H_3+H	9.4E+21	−1.8	346.4	46
90	C_4H_3+M ⇔ C_4H_2+H+M	1.0E+16	0	249.8	46
91	C_2H_2+M ⇔ C_2H+H+M	4.2E+16	0	447.7	46
92	H+H+M ⇔ H_2+M	1.0E+18	−1	0.0	46
93	H+H+H_2 ⇔ H_2+H_2	9.2E+16	−0.6	0.0	46
94	CN+C_2H_3 ⇔ H_2CCHCN	6.3E+13	0	0.0	21
95	CN+C_2H_5 ⇔ C_2H_5CN	3.0E+13	0	0.0	est
96	CH_2CH_2CN ⇔ C_2H_4+CN	1.8E+15	0	251.0	21
97	H_2CCHCN+H ⇔ CH_3CHCN	1.0E+13	0	19.7	21
98	H_2CCHCN+C_2H_3 ⇔ HCCHCN+C_2H_4	5.0E+13	0	33.5	21
99	2HCCHCN ⇔ H_2CCHCN+HCCCN	1.0E+50	−10.5	284.5	21
100	C_2H_5CN ⇔ H+CH_2CH_2CN	1.0E+15	0	410.0	21
101	C_2H_5CN ⇔ H+CH_3CHCN	3.0E+15	0	384.9	21
102	C_2H_5CN+H ⇔ H_2+CH_2CH_2CN	6.3E+13	0	29.3	21
103	C_2H_5CN+H ⇔ H_2+CH_3CHCN	6.3E+13	0	27.6	21
104	C_2H_5CN+H ⇔ HCN+C_2H_5	1.0E+14	0	41.8	21
105	C_2H_5CN+CH_3 ⇔ CH_4+CH_2CH_2CN	1.0E+12	0	33.5	21
106	C_2H_5CN+CH_3 ⇔ CH_4+CH_3CHCN	1.0E+12	0	33.5	21
107	C_4H_5N ⇔ PYRLYL+H	3.0E+15	0	447.7	6
108	H+PYRLNE ⇔ PYRLYL+H_2	6.0E+14	0	50.2	6
109	PYRLYL ⇔ C−C_3H_4CN	3.0E+13	0	163.2	est
110	PYRLNE ⇔ PYRLYL+H	6.3E+14	0	348.9	6
111	SUCC ⇔ H_2CCHCN+HCN	2.9E+14	0	366.1	21
112	CH_3+CH_2CN ⇔ C_2H_5CN	2.0E+13	0	0.0	21
113	CH_2CH_2CN ⇔ H+H_2CCHCN	3.1E+13	0	153.1	21
114	C_3H_4P+M ⇔ C_3H_3+H+M	2.1E+101	−23.1	597.9	40
115	2C_3H_3 ⇔ L−C_6H_6	6.0E+13	0	0.0	est
116	L−C_6H_6 ⇔ C_6H_6	1.0E+12	0	209.2	est
117	CN+C_2H_2 ⇔ HCN+C_2H	5.0E+13	0	20.9	est

[a] ⇔ denotes reversible reaction. Reverse rate constant is calculated from the equilibrium constant. (+M) denotes a reaction in the falloff region; falloff parameters are given in the reference. [b] Units for A are $cm^3\ mol^{-1}\ s^{-1}$ or s^{-1} as appropriate. Units for E_a are kJ mol^{-1}. [c] PW denotes a rate constant determined in the present work. abin denotes a rate constant evaluated by ab initio calculation. est denotes a rate constant estimated in the present work. [d] Value specific to the pressure of 12 atm. [e] High-pressure rate constants $k_{1\infty} = 10^{13.50}T^{0.005}\exp(-193.7/RT)$; $k_{3\infty} = 10^{15.72}\exp(-316.5/RT)$; $k_{4\infty} = 10^{15.52}\exp(-292.8/RT)$; $k_{5\infty} = 10^{15.40}\exp(-332.2/RT)$; $k_{6\infty} = 10^{17.01}\exp(-362.6/RT)$.

Bicyclization of Pyrrole with Subsequent Decomposition to HCN and Propyne. The pyrrolenines were also found to have the capacity to isomerize to the bicyclic forms Py04 and Py05, as indicated in Figure 1. The latter reaction was predicted to have a sufficiently low barrier for it to be considered further, whereby Py05 would decompose to ultimately yield HCN and propyne. A concerted 1,2-H migration (to the nitrogen) and CC bond breaking reaction results in a fairly stable cyclic intermediate Py46, which on ring opening would yield Py25 and subsequently HCN and propyne. The PES of this scheme is shown in Figure 10. According to the G2(MP2) results, however, the first step is far too energetic for this reaction to be of importance. Therefore, the critical energy of the ring-opening step was not determined, as this pathway is not included in the kinetic model.

Kinetic Modeling. Kinetic modeling using the reaction model given in Table 1 was performed using the Sandia CHEMKIN code[32] together with the shock tube code[33] (modified to allow

TABLE 2: Thermochemical Parameters for Important Species in the Pyrrole System

				C_p^0/J K^{-1} mol^{-1}					
name[a]	structure	$\Delta_f H^\circ_{298}$, kJ mol^{-1}	S°_{298}, J K^{-1} mol^{-1}	300	500	1000	1500	2000	ref
C_4H_5N (Py00)	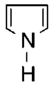	108.3	270.5	71.76	117.2	173.9	198.6	211.0	26/abin
PYRLNE (Py01)		165.9	277.3	70.04	115.0	174.5	200.0	212.2	6/abin
PYRLYL		294.8	274.2	67.49	107.2	156.3	177.7	188.4	6/abin
PYROP (Py10)	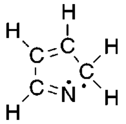	413.1	312.1	91.21	128.9	178.6	201.5	212.9	PW/abin[b]
HNCPROP (Py25)	HN=CH−CH=C=CH_2	287.5	312.5	86.36	123.6	175.8	200.0	212.1	PW/abin[b]
AC_3H_4CN (PL5)	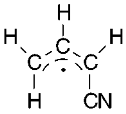	285.5	308.1	86.81	120.0	162.6	181.9	191.5	PW/abin[b]
$C-C_3H_4CN$	$HC^\bullet$=CH−CH_2CN	383.1	335.4	88.20	117.0	156.1	178.9	189.8	29/add[c]
C_3H_4CN	CH_3−CH=$C^\bullet$−CN	355.5	301.8	89.91	119.2	158.2	175.6	187.2	29/add[c]

[a] Name as given in Table 1. (Name as given in figures). [b] Evaluated by ab initio (abin) calculation in the present work (PW). [c] Estimated by group additivity methods in the given reference.

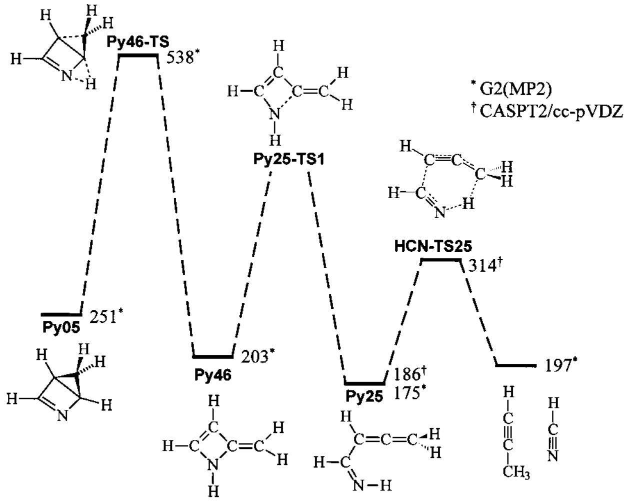

Figure 10. Potential energy surface for the formation of HCN and propyne from the bicyclic isomer Py05 at 0 K. (Energies in kJ mol^{-1} relative to pyrrole.)

for cooling by the reflected rarefaction wave) and the ordinary differential equation solver LSODE.[34] Thermodynamic data for key species of the pyrrole system are given in Table 2. Predicted decomposition and product profiles are compared with experimental data[4] in Figure 11. Rate sensitivity analysis was carried out on the model using the SENKIN[35] code. Many of the key reactions in the model have been evaluated from ab initio calculations as described above. In general, reverse rate constants have been evaluated using the equilibrium constants that have been calculated from the thermochemistry by standard methods.

According to the model, pyrolysis is preceded by the rapid reversible tautomerization to pyrrolenine (2*H*-pyrrole) (reaction 1 of Table 1). The high-pressure rate constant for this reaction has been taken directly from the ab initio calculations. For the average pressure of 12 atm at which the experimental results were obtained,[4] this reaction is slightly into the falloff regime, hence an RRKM falloff calculation has been made and the specific rate constant is given in Table 1. Further rearrangement of the 2*H*-pyrrole to 3*H*-pyrrole may also take place as shown in Figure 1 but, as this rearrangement does not lead to new products, it has not been included in the modeling. Pyrolysis then takes place simultaneously through the cyclic carbene route, leading to the intermediate Py25 (reaction 2) and by fission of the considerably weaker C−N bond in pyrrolenine to biradical Py10 as shown by the potential energy surface depicted in Figure 2. There is also a small barrier (~6 kJ mol^{-1}) to closure of the biradical. RRKM analysis revealed that reaction 2 is essentially at the high-pressure limit over the entire range of temperatures studied.

Using the CASSCF/cc-pVDZ geometries and frequencies for transition state and pyrrolenine, we calculate a rate constant for pyrrolenine → biradical Py10 of $6.7 \times 10^{14} \exp(-254\ \text{kJ mol}^{-1}/RT)\ \text{s}^{-1}$, thermally corrected to an average temperature of 1500 K. The transition states for rearrangement of the biradical to allyl cyanide and to *cis*-crotononitrile have quite low barriers (see Figure 4) and the rate constants for formation of these isomers of pyrrole when calculated at 1500 K from the ab initio geometries and frequencies are $1.1 \times 10^{13} \exp(-59\ \text{kJ mol}^{-1}/RT)\ \text{s}^{-1}$ and $8.2 \times 10^{12} \exp(-32\ \text{kJ mol}^{-1}/RT)\ \text{s}^{-1}$, respectively, using the (CASPT2/cc-pVDZ) critical energies. As discussed above, the biradical can also undergo transfer of a hydrogen atom to form the stable allenic imine (Py25). The critical energy for this transfer is approximately 70 kJ mol^{-1}, and the rate constant at 1500 K derived from the CASPT2/cc-pVDZ calculations is $5.2 \times 10^{12} \exp(-74\ \text{kJ mol}^{-1}/RT)\ \text{s}^{-1}$. A further relatively low-energy mode of decomposition of the biradical is to form cyanoallyl + H, as discussed above, for which the rate constant of $6.5 \times 10^{13} \exp(-108\ \text{kJ mol}^{-1}/RT)\ \text{s}^{-1}$ was also calculated from the CASPT2/cc-pVDZ results.

Our preliminary approach to kinetic modeling was first to consider that biradical Py10 was stabilized and to treat its decomposition via the four low-energy channels, viz., to allyl cyanide, *cis*-crotononitrile, HCN + propyne and to cyanonallyl + H. The derived rate constants for the first three processes at the experimental temperatures studied would actually exceed $10^9\ \text{s}^{-1}$. This value, as pointed out recently by Kiefer[36] exceeds the largest rate that can be supported by collisional activation in argon. Use of these very large rate constants in the kinetic model led to a far too rapid decomposition of pyrrole. When

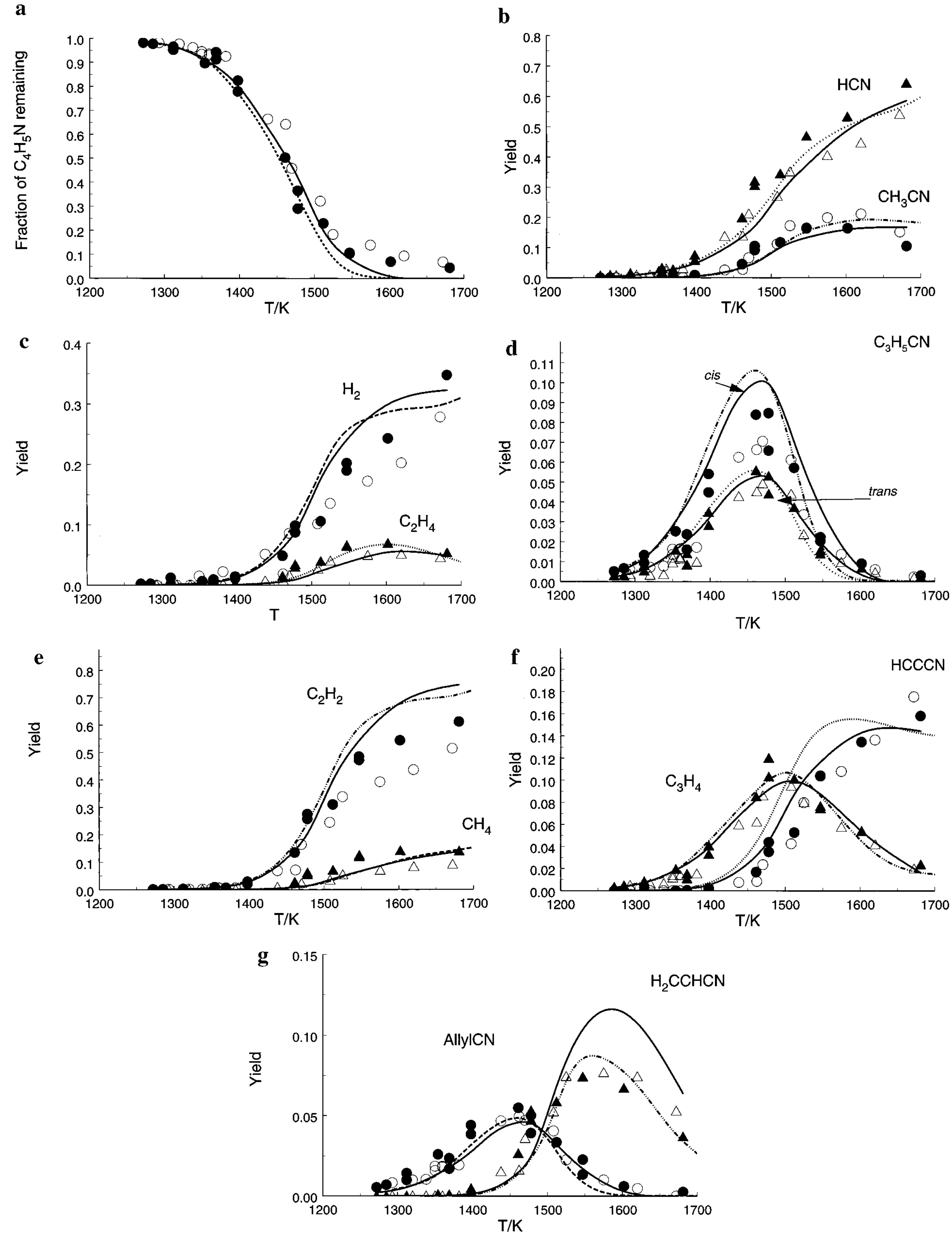

Figure 11. Temperature dependence of designated species in the pyrolysis of pyrrole (filled symbols = data points at initial pyrrole concentration of 0.5%, open symbols = data points at initial pyrrole concentration of 0.075% (both sets from ref 14), solid lines = model prediction for 0.5%, broken lines = model prediction for 0.075%).

falloff in the rate constants of these four decomposition channels was taken into account, the decomposition became much too slow. This led us to reappraise the assumption of stabilization of the biradical into such a small well. QRRK analysis[37] indicated that there was essentially no stabilization of the biradical; hence the model chosen was that of a four-channel decomposition of pyrrolenine, recalculating the rate constants for each channel from the frequencies and geometries of the respective transition states and of pyrrolenine and barrier heights with respect to pyrrolenine. These are reactions 3−6, respec-

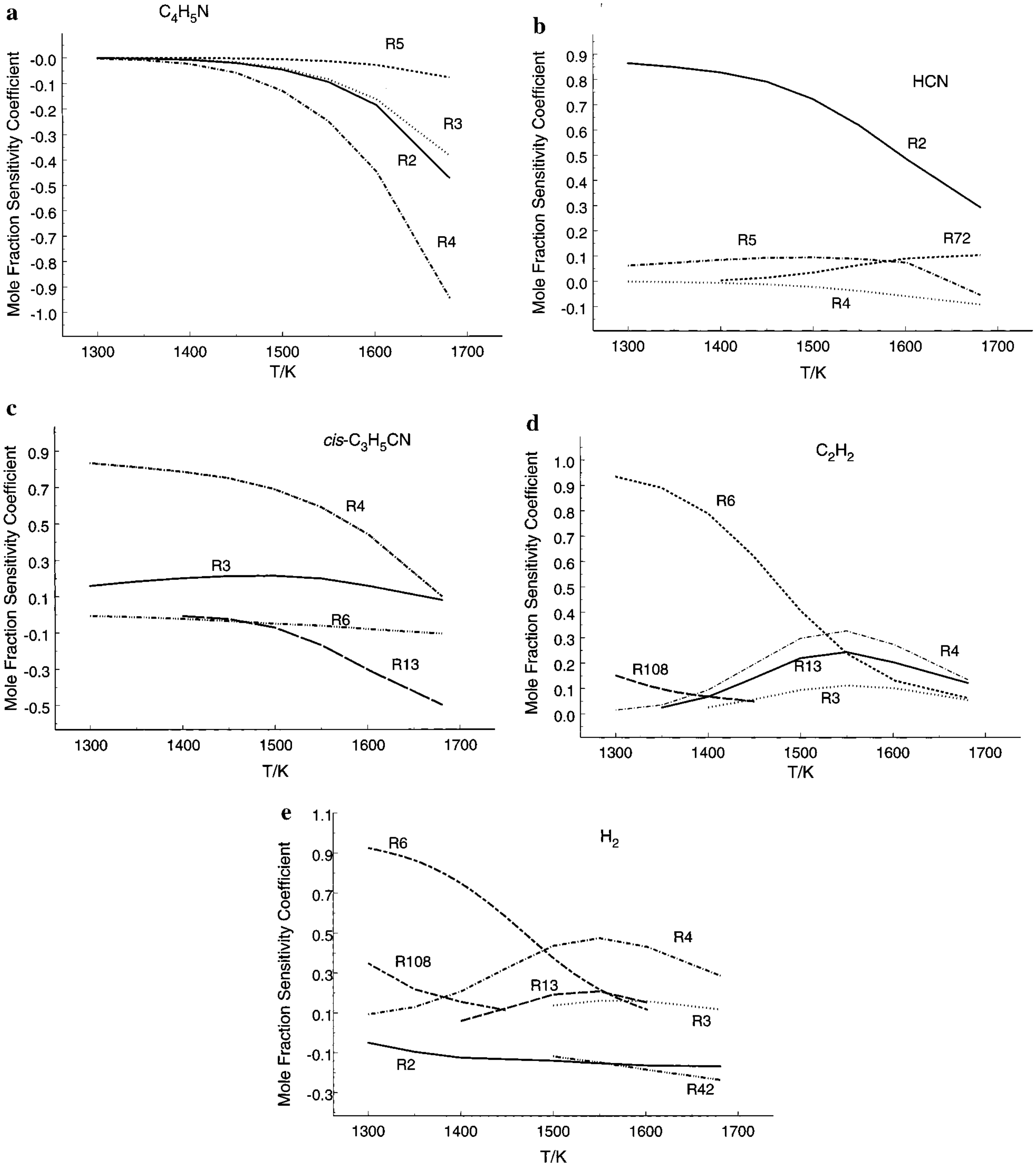

Figure 12. Variation with temperature of sensitivity coefficients for the designated species. Only the most sensitive reactions are shown. Reaction numbers are given in Table 1.

tively, of Table 1. Sensitivity analysis (see below) indicated that these reactions were very sensitive, and it was found that use of the higher critical energies as calculated by the G2(MP2) method when the high-pressure rate constants for reactions 3 and 4 were calculated gave much better agreement with experiment. It was found necessary to increase the activation energy for reaction 6 by 8 kJ mol^{-1}. The critical energy for this reaction was calculated by the CASPT2/VTZ2P method, and this adjustment is considered to be within the possible error bounds of the ab initio calculations. Rate constants for reactions 3−6 are slightly into the falloff regime so that pressure-specific rate constants are given in Table 1 for these reactions.

HCN and propyne arise from the concerted H transfer and bond fission reaction of Py25 (reaction 7) and the rate constant for this is taken directly from the ab initio calculations.

The pyrrole isomers *cis*- and *trans*-crotononitrile and allyl cyanide are important products that, however, also undergo thermal decomposition in the same temperature range as pyrrole. Thus, the reaction model contains a subset of the butenenitrile pyrolysis reactions,[29] essentially as presented earlier but with some updated thermochemistry. These reactions comprise reactions 8−41 and 47−52. We did not locate a potential surface for direct conversion of biradical Py10 into *trans*-crotononitrile. Instead, we believe that the pathway to this isomer is as shown in Figure 9. Rate constants for isomerization between the three butenenitrile isomers have been obtained directly from the ab initio calculations.

Acetonitrile is also an important secondary product, and the model contains a submodel for acetonitrile pyrolysis.[21] This submodel also includes pyrolysis mechanisms for acrylonitrile and cyanoacetylene. These are reactions 42−46, 52−106, and 112−114.

In our earlier ab initio study[6] of the NH bond energy in pyrrole we showed that because the ground state of the pyrrolyl radical does not correlate with that of pyrrole, there is a very large barrier to NH fission in the latter. The rate constant for this process is given in Table 1 for reaction 107. Furthermore, pyrrolyl forms mainly from pyrrolenine by reactions 108 and 110 (H abstraction and C−H fission of pyrrolenine). Rate constants for these reactions are taken from our earlier study.

Finally, as benzene is only a minor product of the pyrolysis, we have only included a very rudimentary model of its formation from propargyl radicals (reactions 115 and 116).

Comparison between predicted and experimental profiles for the fraction of pyrrole remaining and of the yields of the major products indicates that there is satisfactory agreement. In general, the model predicts species profiles to within 20−30% over the studied temperature range for two series of initial pyrrole concentrations—namely 5000 and 750 ppm. Only for acrylonitrile, and then only for one initial pyrrole concentration, do the predicted and experimental profiles differ by more than the above. The present modeling represents a significant improvement over our earlier model,[4] especially at the lower end of the temperature scale and can also model *cis*- and *trans*-crotononitrile individually (these were combined in the earlier model).

Rate sensitivity and reaction flux analysis has been carried out on the kinetic model. Variation of sensitivity coefficients for major species is shown in Figure 12. Reaction 1 does not show any sensitivity over the entire range of temperature. On the other hand, flux analysis clearly indicates that this reaction equilibrates rapidly at all temperatures studied. Thus, pyrrolenine is always equilibrated with pyrrole. Reactions 2−6, however, are very sensitive reactions and principally determine the rate of disappearance of pyrrole. As might be expected, the most sensitive reactions for formation of allyl cyanide and *cis*-crotononitrile are reactions 3 and 4. (Sensitivity coefficients are only shown for *cis*-crotononitrile. Sensitivities for allyl cyanide and *trans*-crotononitrile are very similar to those for *cis*-crotononitrile.) The most sensitive reaction for formation of HCN is reaction 2. Reaction 6, reaction to fission off a H atom and produce cyanoallyl, is the most sensitive reaction for formation of C_2H_2, H_2, CH_3CN, and H_2CCHCN. This is because the cyanoallyl radical, AC_3H_4CN, is an important precursor for production of C_2H_2 because AC_3H_4CN can rearrange to the nonallylic $C-C_3H_4CN$ (reaction 26) followed by fission into $C_2H_2 + CH_2CN$. The cyanomethyl radical so produced then gives rise to CH_3CN principally via reaction −42, recombination with H atom. At higher temperatures, the decomposition reaction of allyl cyanide (reaction −13) also becomes important for production of acetonitrile. Reaction 6 is also the principal source of H atoms at the lowest temperatures, so that most flux to molecular hydrogen passes through this route, hence the high sensitivity of H_2 to reaction 6. Initially, reaction 108, abstraction by H from pyrrolenine, shows some sensitivity for production of H_2.

Lifshitz et al.[3] reported apparent activation energies of formation of certain products of pyrolysis of pyrrole. These were obtained by regression analysis of plots of $\ln\{[\text{product}_i]_{t'}/([\text{pyrrole}]_{t=0}t')\}$, $t' = t_{\text{res}}$, versus $1/T$, where t_{res} is the residence time behind the reflected shock. This approximate relation holds only for small extents of decomposition of initial reactant. We have also used this relation to obtain apparent activation energies of product formation using modeled concentrations at 50 μs after the reflected shock front when the extent of decomposition of initial pyrrole is small. With the exception of HCN, all the plots of apparent activation energy of formation show curvature, at least for temperatures above about 1400 K. If we take the limiting low-temperature slopes of these plots, our activation energies may be compared with those of Lifshitz et al.[3] in Table 3. Agreement may be seen to be reasonable.

TABLE 3: Comparison between Modeled and Experimental[3] Arrhenius Activation Energies of Formation of Products[a]

product	E_a(model), kJ mol^{-1}	E_a(expt), kJ mol^{-1}
HCN	325	351
cis-crotononitrile	291	301[b]
allyl cyanide	344	322
propyne	316	305[c]

[a] Only products whose apparent rate of formation is essentially Arrhenius are tabulated. [b] Data given for *cis*- + *trans*- crotononitrile. [c] Data given for propyne + allene.

Conclusions

Ab initio calculations reveal that pyrrole readily undergoes tautomerization to form the 2*H*- and 3*H*-pyrroles prior to any thermal decomposition. Isomerization and subsequent decomposition is preceded by C−N ring scission in 2*H*-pyrrole (pyrrolenine) to form a biradical (Py10). Four low-energy pathways have been identified arising from this biradical. Two of these lead to the isomerization products, *cis*-crotononitrile and allyl cyanide. A third involving the fission of a H atom and formation of the cyanoallyl radical leads to the products H_2, C_2H_2, acetonitrile, and acrylonitrile. The fourth channel involves the formation of an intermediate allylic imine that is a precursor of HCN and propyne. This last channel is not, however, the principal route to HCN and propyne. Instead, a direct route from pyrrole via a cyclic carbene has been identified as the principal low-energy route to HCN and propyne. A kinetic model with rate constants of key reactions derived from the ab initio calculations has been developed to model pyrolysis data[4] at two initial concentrations of pyrrole. Given that these channels have comparable energetics (as well as Arrhenius parameters) and are hence simultaneously active over a considerable range of temperatures, a realistic description of the pyrolysis process requires the inclusion of all these channels in the kinetic model.

Acknowledgments. We are grateful to Dr Emi Ikeda for carrying out some RRKM calculations. We acknowledge the financial support of the Australian Research Council. M.M. acknowledges the award of an AusAid scholarship.

Supporting Information Available: Tables of optimized geometries, energies, and rotational constants and vibrational frequencies. This material is available free of charge via the Internet at http://pubs.acs.org.

References and Notes

(1) Axworthy, A. E.; Dayan, V. H.; Martin, G. B. *Fuel* **1978**, *57*, 29.

(2) Bruinsma, O. S. L.; Tromp, P. J. J.; de Sauvage Nolting, H. J. J.; Montijn, J. A. *Fuel* **1988**, *67*, 334.

(3) Lifshitz. A.; Tamburu. C.; Suslensky, A. *J. Phys. Chem.* **1989**, *93*, 5802.

(4) Mackie, J. C.; Colket, M. B.; Nelson, P. F.; Esler, M. *Int. J. Chem. Kinet.* **1991**, *23*, 733.

(5) Benson, S. W. *Thermochemical Kinetics*; John Wiley: New York, 1976.

(6) Bacskay, G. B.; Martoprawiro, M.; Mackie, J. C. *Chem. Phys. Lett.* **1998**, *290*, 391.

(7) Bacskay, G. B.; Martoprawiro, M.; Mackie, J. C. *Chem. Phys. Lett.* **1999**, *300*, 321.

(8) Roos, B. O.; Taylor, P. R.; Siegbahn, P. E. S. *Chem. Phys.* **1980**, *48*, 157.

(9) Roos, B. O. In *Ab Initio Methods in Quantum Chemistry-II*; Lawley, K. P., Ed.; J. Wiley & Sons Ltd., Chichester, U.K., 1987; p 399.

(10) Dunning, T. H., Jr. *J. Chem. Phys.* **1989**, *90*, 1007.

(11) Andersson, K.; Malmqvist, P-Å.; Roos, B. O.; Sadlej, A. J.; Wolinski, K. *J. Phys. Chem.* **1990**, *94*, 5483.

(12) Andersson, K.; Malmqvist, P-Å.; Roos, B. O. *J. Chem. Phys.* **1992**, *96*, 1218.

(13) Curtiss, L. A.; Raghavachari K.; Pople, J. A. *J. Chem. Phys.* **1993**, *98*, 1293.

(14) McQuarrie, D. A. Statistical Mechanics (Harper & Row: New York, 1973) p 129.

(15) Steinfeld, J. I.; Francisco, J. S.; Hase, W. L. *Chemical Kinetics and Dynamics*; Prentice Hall Inc.: Englewood Cliffs, NJ, 1989; p 308.

(16) "DALTON, an ab initio electronic structure program, Release 1.0 1997" written by T. Helgaker, H. J. Aa. Jensen, P. Joergensen, J. Olsen, K. Ruud, H. Aagren, T. Andersen, K. L. Bak, V. Bakken, O. Christiansen, P. Dahle, E. K. Dalskov, T. Enevoldsen, B. Fernandez, H. Heiberg, H. Hettema, D. Jonsson, S. Kirpekar, R. Kobayashi, H. Koch, K. V. Mikkelsen, P. Norman, M. J. Packer, T. Saue, P. R. Taylor, and O. Vahtras.

(17) Andersson, K.; Blomberg, M. R. A.; Fülscher, M. P.; Kellö, V.; Lindh, R.; Malmqvist, P-Å.; Noga, J.; Olsen, J.; Roos, B. O.; Sadlej, A. J.; Siegbahn, P. E. M.; Urban, M.; Widmark, P.-O. *MOLCAS version 2*; University of Lund: Lund, Sweden, 1997.

(18) Andersson, K.; Blomberg, M. R. A.; Fülscher, M. P.; Karlström, G.; Lindh, R.; Malmqvist, P.-Å.; Neogrády, P.; Olsen, J.; Roos, B. O.; Sadlej, A. J.; Schütz, M.; Seijo, L.; Serrano-Andrés, L.; Siegbahn, P. E. M.; P.-O. Widmark, *MOLCAS Version 4*; Lund University: Lund, Sweden, 1993.

(19) Frisch, M. J.; Trucks, G. W.; Schlegel, H. B.; Gill, P. M. W.; Johnson, B. G.; Robb, M. A.; Cheeseman, J. R.; Keith, T.; Petersson, G. A.; Montgomery, J. A.; Raghavachari, K.; Al-Laham, M. A.; Zakrzewski, V. G.; Ortiz, J. V.; Foresman, J. B.; Cioslowski, J.; Stefanov, B. B.; Nanayakkara, A.; Challacombe, M.; Peng, C. Y.; Ayala, P. Y.; Chen, W.; Wong, M. W.; Andres, J. L.; Replogle, E. S.; Gomperts, R.; Martin, R. L.; Fox, D. J.; Binkley, J. S.; Defrees, D. J.; Baker, J.; Stewart, J. P.; Head-Gordon, M.; Gonzalez, C.; Pople, J. A. *Gaussian 94*, Revision E.2; Gaussian, Inc.: Pittsburgh, PA, 1995.

(20) Frisch, M. J.; Trucks, G. W.; Schlegel, H. B.; Scuseria, G. E.; Robb, M. A.; Cheeseman, J. R.; Zakrzewski, V. G.; Montgomery, J. A.; Stratmann, R. E.; Burant, J. C.; Dapprich, S.; Millam, J. A.; Daniels, A. D.; Kudin, K. A.; Strain, M. C.; Farkas, O.; Tomasi, J.; Barone, V.; Cossi, M.; Cammi, R.; Mennucci, B.; Pomelli, C.; Adamo, C.; Clifford, S.; Ochterski, J.; Petersson, G. A.; Ayala, P. Y.; Cui, Q.; Morokuma, K.; Malick, D. K.; Rabuck, A. D.; Raghavachari, K.; Foresman, J. B.; Cioslowski, J.; Ortiz, J. V.; Stefanov, B. B.; Liu, G.; Liashenko, A.; Piskorz, P.; Komaromi, I.; Gomperts, R.; Martin, R. L.; Fox, D. J.; Keith, T.; Al-Laham, M. A.; Peng, C. Y.; Nanayakkara, A.; Gonzalez, C.; Challacombe, M.; Gill, P. M. W.; Johnson, B. G.; Chen, W.; Wong, M. W.; Andres, J. L.; Head-Gordon, M.; Reploge, E. S.; Pople, J. A. *Gaussian 98*, Revision A.3; Gaussian, Inc.: Pittsburgh, PA, 1998.

(21) Sendt, K.; Ikeda, E.; Bacskay, G. B.; Mackie, J. C. *J. Phys. Chem. A* **1999**, *103*, 1054.

(22) Chase, M. W.; Davies, C. A.; Downey, J. R.; Frurip, D. J.; McDonald, R. A.; Syverud, A. N. *J. Phys. Chem. Ref. Data* **1985**, *14*, Suppl. 1, 1.

(23) Tsang, W. In *Heats of Formation of Organic Free Radicals by Kinetic Methods in Energetics of Organic Free Radicals*; Martinho Simoes, J. A., Greenberg, A., Liebman, J. F., Eds.; Blackie: London, 1996; p 22.

(24) Konicek, J.; Prochazka, M.; Krestanova, V.; Smisek, M. *Collect. Czech. Chem. Commun*. **1969**, *34*, 2249.

(25) Furayama, S.; Golden, D. M.; Benson, S. W. *J. Chem. Thermodyn.* **1969**, *1*, 363.

(26) Scott, D. W.; Berg, W. T.; Hossenlopp, I. A.; Hubbard, W. N.; Messerly, J. F.; Todd, S. S.; Douslin, D. R.; McCullough, J. P.; Waddington, G. *J. Phys. Chem*. **1967**, *71*, 2263.

(27) Wyss, H. R.; Gunthard, H. H. *Helv. Chim. Acta* **1961**, *44*, 625.

(28) Dubnikova, F.; Lifshitz, A. *J. Phys. Chem. A* **1998**, *102*, 10880.

(29) Doughty, A.; Mackie, J. C. *J. Phys. Chem.* **1992**, *96*, 272.

(30) Luckraft, D. A.; Robinson, P. J. *Int. J. Chem. Kinet*. **1973**, *5*, 137.

(31) Dubnikova, F.; Lifshitz, A. *J. Phys. Chem. A* **1998**, *102*, 5876.

(32) Kee, R. J.; Miller, J. A.; Jefferson, T. H. "CHEMKIN; A General Purpose, Problem Independent, Transportable FORTRAN Chemical Kinetics Code Package. SANDIA National Laboratories Report SAND80-003, March, 1980.

(33) Mitchell, R. E.; Kee, R. J. A General Purpose Computer Code for Predicting Chemical Kinetic Behavior Behind Incident and Reflected Shocks. SANDIA National Laboratories, SAND82-8205, March, 1982.

(34) Hindmarsh, A. C. LSODE and LSODI: Two New Initial Value Differential Equation Solvers. *ACM Signum Newsletter* **1980**, *15* (4).

(35) Lutz, A. E.; Kee, R. J.; Miller, J. A. SENKIN: A FORTRAN Program Predicting Homogeneous Gas-Phase Chemical Kinetics with Sensitivity Analysis. SANDIA National Laboratories Report SAND87-8248, February, 1988.

(36) Kiefer, J. H. Some Unusual Aspects of Unimolecular Falloff of Importance in Combustion Modeling. Invited topical review to 27th International Symposium on Combustion, The Combustion Institute, Pittsburgh, PA, 1998; p 113.

(37) Dean, A. M. *J. Phys. Chem.* **1985**, *89*, 4600. Westmoreland, P. R.; Howard, J. B.; Longwell, J. P.; Dean, A. M. *AIChE J.* **1986**, *32*, 1971.

(38) Hidaka, Y.; Nakamura, T.; Miyauchi, A.; Shiraishi, T.; Kawano, H. *Int. J. Chem. Kinet.* **1989**, *21*, 643.

(39) Kerr, J. A.; Parsonage, M. J. *Evaluated Kinetic Data on Gas-Phase Addition Reaction: Reactions of Atoms and Radicals with Alkenes, Alkynes and Aromatic Compounds*; Butterworths: London, 1972.

(40) Mallard, W. G.; Westley, F.; Herron, J. T.; Hampson, R. G.; Frizzell, D. H. NIST Chemical Kinetic Database, Version 6.0; National Institute of Standards and Technology: Gaithersburg, MD, 1994.

(41) Kiefer, J. H.; Mitchell, K. I.; Kern, R. D.; Yong, J. N. *J. Phys. Chem.* **1988**, *92*, 2, 677.

(42) Warnatz. J. In *Combustion Chemistry*; Gardiner, W. C., Jr., Ed.; Springer: New York, 1984; p 197.

(43) Weissman, M. A.; Benson, S. W. *J. Phys. Chem.* **1988**, *92*, 4080.

(44) Payne, W. A.; Stief, L. J. *J. Chem. Phys.* **1976**, *64*, 1150.

(45) Miller, J. A.; Bowman, C. T. *Prog. Energy Combust. Sci.* **1989**, *15*, 287.

(46) Bowman, C. T.; Hanson, R. K.; Davidson, D. F.; Gardiner, W. C.; Lissianski, V.; Smith, G. P.; Golden, D. M.; Frenklach, M.; Goldenberg, M. GRIMech: *http://www.me.berkeley.edu/gri_mech.*